Late Quaternary characteristics of the northern Embudo fault, Taos County, New Mexico

K. I. Kelson, P. W. Bauer, J. R. Unruh, and J. D. J. Bott, 2004, pp. 147-157

in:

Geology of the Taos Region, Brister, Brian; Bauer, Paul W.; Read, Adam S.; Lueth, Virgil W.; [eds.], New Mexico Geological Society 55th Annual Fall Field Conference Guidebook, 440 p.

This page is intentionally left blank to maintain order of facing pages.

LATE QUATERNARY CHARACTERISTICS OF THE NORTHERN EMBUDO FAULT, TAOS COUNTY, NEW MEXICO

KEITH I. KELSON[1], PAUL W. BAUER[2], JEFFREY R. UNRUH[1], AND JACQUELINE D.J. BOTT[3]
[1]William Lettis & Associates, Inc., 1777 Botelho Drive, Suite 262, Walnut Creek, CA 94596
[2]New Mexico Bureau of Geology and Mineral Resources, 801 Leroy Place, Socorro, NM 87801
[3]California Geological Survey, 185 Berry Street, San Francisco, CA 95814

ABSTRACT.—The seismic potential of transfer fault zones in active rifts is poorly understood, with no known historical examples of surface-rupturing earthquakes along structures that trend obliquely across rifts. The Embudo fault, which is a transfer zone that strikes N60˚E across the north-trending Rio Grande rift, accommodates differential movement between the east-tilted San Luis Basin on the north and the west-tilted Española Basin on the south. Detailed geologic mapping along the northeastern 18 km of the Embudo fault provides evidence of late Pleistocene and possibly Holocene displacement along many discontinuous fault strands that are distributed over a width of several kilometers. The northeastern part of the Embudo fault has had left-oblique slip during the late Quaternary, as suggested by substantial along-strike variations in scarp heights, subhorizontal slickensides on fault planes, and reverse faulting within a right step-over. Fault-scarp heights along the northeastern part of the Embudo fault appear to correlate more with local strikes of fault strands than with age. The fault strands with northeasterly strikes exhibit prominent scarps, and strands with more westerly strikes have low scarps and subtle geomorphic expression. In comparison, the north-striking, rift-margin Sangre de Cristo fault, directly north of the Embudo fault, has prominent, continuous geomorphic expression and well-defined scarps suggesting late Pleistocene and possibly Holocene activity. These relations are consistent with roughly east-west extension across the rift, and left-lateral slip on the northeast-striking northeastern section of the Embudo fault, rather than reverse slip as previously postulated based on limited roadcut exposures. It is unclear whether the Embudo fault is an independent or dependent seismic source, although evidence of late Pleistocene and possibly Holocene activity on the northeastern section of the Embudo fault suggests that it should be considered as an independent seismogenic source.

INTRODUCTION

The Rio Grande rift in northern New Mexico contains many potentially active seismogenic sources, with numerous faults exhibiting evidence of late Pleistocene or Holocene movement (Machette and Personius, 1984; Gardner and House, 1987; Menges, 1988, 1990; Wong et al., 1996; Machette et al., 1998; Gardner et al., 2003). Because most of these faults are poorly studied, regional seismic hazard analyses must estimate the characteristics of many potential seismic sources through analogy with similar structures. In particular, the seismic potential of transfer fault zones, such as the Embudo fault, is poorly understood, with no known historical examples of surface-rupturing earthquakes along structures that trend obliquely across rifts. The Embudo fault strikes N60˚E across the north-trending Rio Grande rift and accommodates differential extensional movement between the east-tilted San Luis Basin on the north and the west-tilted Española Basin on the south. This paper provides an initial characterization of the northeastern part of the Embudo fault, and addresses the fault's seismic potential and role in the late Quaternary tectonic setting of the Rio Grande rift.

The 65-km-long Embudo fault forms the structural boundary between two actively subsiding asymmetric grabens: the east-tilted San Luis Basin, which is bordered on the east by the west-dipping Sangre de Cristo fault; and the west-tilted northern Española Basin, which is bordered on the west by the east-dipping Pajarito fault (Fig. 1). The Embudo fault has been characterized as a transfer (or accommodation) zone (Rosendahl, 1987; Faulds and Varga, 1998) that allows differential subsidence between rift basins (Muehlberger, 1979). Machette et al. (1998) identified two primary sections of the fault: (1) a southwestern section that extends from Clara Peak on the south to the village of Embudo, and (2) a northeastern section from Embudo on the south to near the village of Ranchos de Taos on the north (Fig. 1). Numerous regional to outcrop-scale studies have shown that the northeastern fault section was dominated by left-lateral strike-slip since the late Tertiary (Steinpress, 1981; Leininger, 1982; Hillman, 1986; Hall, 1988; Bradford, 1992). However, there are no well-constrained data on the late Quaternary sense and rate of slip, or

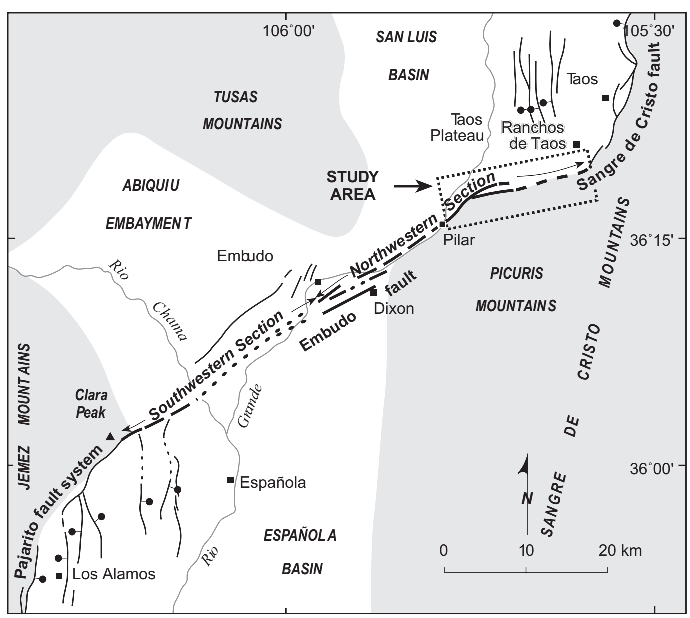

FIGURE 1. Regional fault map showing northern and southern sections of the Embudo fault, and the area mapped for this study. Direction of regional extension shown by large arrows.

on the number, timing, and recurrence of large earthquakes along the Embudo fault. These data are critical for evaluating seismic hazard in the northern Rio Grande rift, for assessing the present-day regional seismotectonic setting, and for characterizing fault segmentation and possible rupture scenarios. An improved understanding of the seismic potential and kinematic role of the Embudo fault in accommodating extension in the northern Rio Grande rift is essential for assessing the pattern of active deformation in northern New Mexico.

This research concentrated on mapping and characterizing the late Quaternary strands of the northeastern 18 km of the Embudo fault, along the northern margin of the Picuris Mountains between the towns of Pilar and Ranchos de Taos (Fig. 1). The purposes of this paper are to provide information on the location, timing, and style of late Quaternary deformation along the northeastern section of the Embudo fault, and to address the role of the northeastern Embudo fault in the late Quaternary tectonics of the northern Rio Grande rift.

PATTERN OF LATE QUATERNARY DEFORMATION

We mapped late Quaternary strands of the Embudo fault through analysis of 1970s-vintage color aerial photography and detailed field studies (Kelson et al., 1997a; Bauer and Kelson, 1997; Kelson and Bauer, 1998, 2003; Bauer et al., 1999). We also developed detailed maps of late Quaternary surficial deposits along the Picuris Mountains piedmont, which allowed us to assess the relative age and character of fault strands. Surficial deposits traversed by the northeastern 18 km of the Embudo fault are primarily Pleistocene alluvial-fan deposits shed to the north from the Picuris Mountains. These fan deposits interfinger with alluvium flanking the Rio Pueblo de Taos and Rio Grande to the north and northwest, respectively, and are inset by Holocene alluvium along active arroyos.

The northeastern 18 km of the Embudo fault exhibits a complex pattern of deformation. The distribution and abundance of topographic scarps, vegetation lineaments, and tonal air-photo contrasts associated with the fault varies considerably along strike, with geomorphic evidence present on several different surficial deposits along the fault. Scarp heights on similar-aged deposits vary substantially along the fault, but there are no obvious relations among scarp height, age of faulted deposit, and location along the fault. However, our mapping suggests that the Embudo fault between Pilar and Talpa can be divided into four distinct local fault reaches (Fig. 2) characterized by different geomorphic features that we interpret to reflect the style of deformation. We infer that the characteristics of these reaches are related to the local sense of slip and to fault complexities along strike. In general, it appears that the eastern reach (reach A) has had a relatively large component of northwest-down normal slip, the east--central reach (reach B) is characterized by a large component of left-lateral slip, the west-central reach (reach C) is characterized by reverse faulting related to a restraining step-over in the lateral-slip fault, and the western reach (reach D) is characterized by northwest-down, left-normal oblique slip.

Reach A (La Serna Grant)

This 7-km-long reach extends southwestward from the southern Sangre de Cristo fault (the Cañon section of Machette et al., 1998) near the village of Talpa (Fig. 2). This fault intersection generally delineates the physiographic boundary between the Taos Plateau, the Sangre de Cristo Mountains, and the Picuris Mountains (Fig. 1). The western end of the reach coincides with the north-striking Picuris-Pecos fault (Bauer, 1988; Bauer and Kelson, 1997). The overall strike of reach A is N65˚E, which is more easterly than the N40˚E-striking Cañon section of the Sangre de Cristo fault to the north. Fault strands along reach A are geomorphically well expressed as scarps across alluvial-fan deposits, prominent topographic breaks at the bases of triangular hill-front facets, and tonal lineaments on aerial photographs. Although in places there are multiple anastomosing fault strands, the fault can be mapped continuously in surficial deposits along the entire reach (Bauer and Kelson, 1997). Early Pleistocene alluvial-fan deposits (unit Qf1; Figure 3) along reach A have about 10 m of northwest-down net vertical tectonic displacement (NVTD). A re-worked ash sampled from these deposits yielded an age of 1.27 ± 0.02 Ma ($^{40}Ar/^{39}Ar$ method, W. McIntosh, personal commun., 1996; Bauer and Kelson, 1997). Middle Pleistocene alluvial-fan deposits (unit Qf2) along this reach have about 4 m of northwest-down NVTD, and middle to late Pleistocene fan deposits (unit Qf3) have about 2 m of northwest-down NVTD along this reach. Latest Pleistocene to Holocene alluvial-fan deposits (unit Qfy) exhibit subtle vegetation lineaments where crossed by fault strands but have no prominent topographic scarps.

Reach B (Gijosa Grant)

This 7-km-long reach extends southwestward from Arroyo del Alamo, along the northern flank of the Picuris Mountains, to Arroyo Hondo (Fig. 2). The eastern boundary of this reach roughly coincides with the northern end of the Picuris-Pecos fault. The overall strike of reach B is N85˚E, which is more easterly than the N65˚E-striking reach A described above. Reach B has poor geomorphic expression, although the presence of several alluvial-fan and stream-terrace deposits along the mountain front would be expected to preserve evidence of vertical displacement (Kelson et al., 1997a; Bauer and Kelson, 1997). A few discontinuous topographic scarps and tonal lineaments on early Pleistocene alluvial-fan deposits (units Qfo and Qf1) suggest complex faulting within a zone as much as 3 km wide north of the mountain front. Topographic profiles across these early Pleistocene deposits show lower amounts of north-down NVTD than profiles across younger deposits in reach A, suggesting a lower slip rate or a significant component of lateral offset along the fault.

Reach C (Arroyo Hondo Area)

This 2-km-long reach near Arroyo Hondo shows a complex pattern of deformation consisting of three major strands within a 1.5-km-wide zone. The southern fault strand lies within Precambrian rocks of the Picuris Mountains and is not exposed in any of

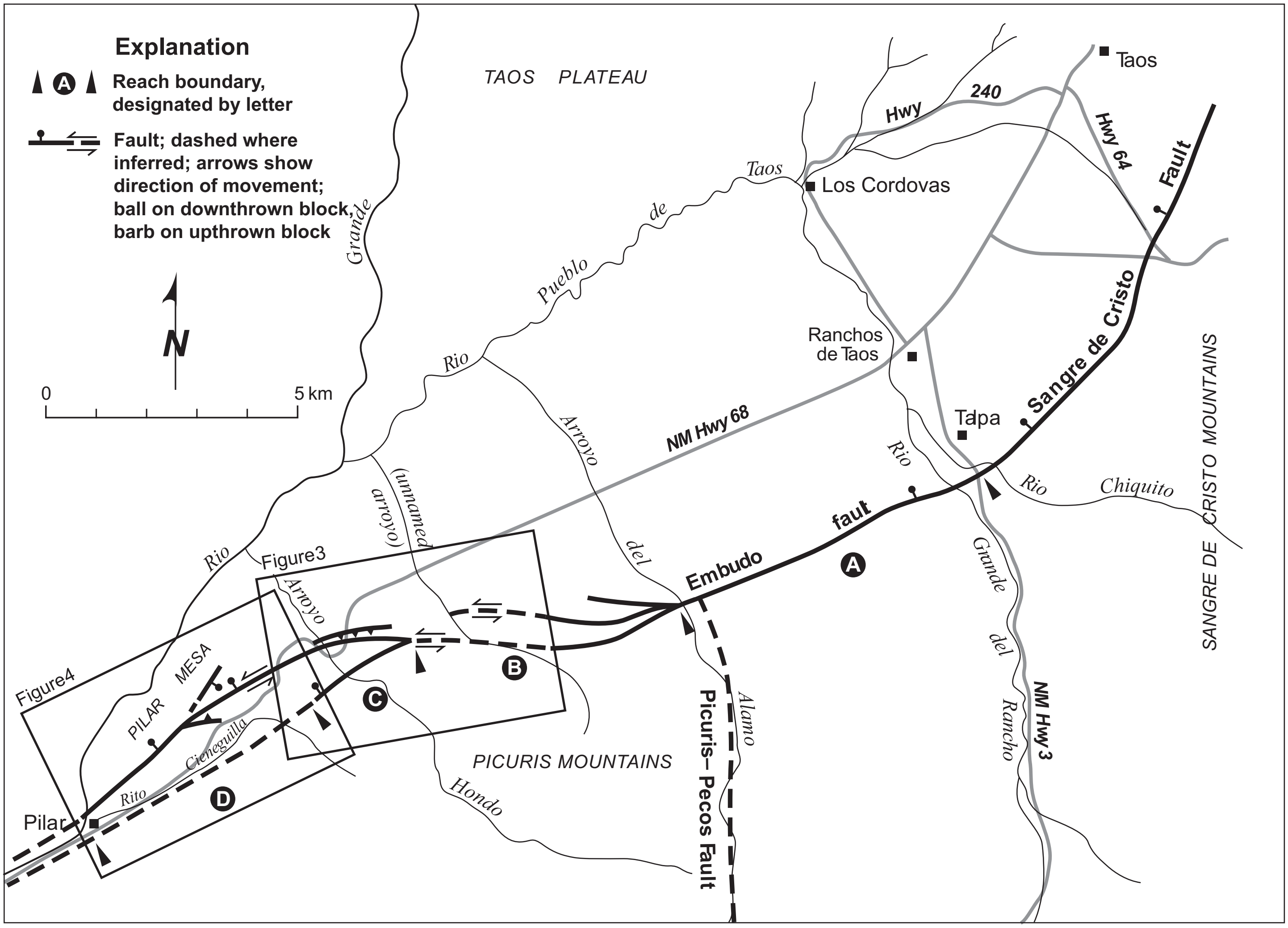

FIGURE 2. Simplified map of the Embudo fault between Pilar and Talpa, showing local fault reaches A through D. The Sangre de Cristo fault extends northward from Talpa to Poncha Pass, Colorado, beyond the figure boundary.

the roadcuts along NM-68 (Bauer and Kelson, 1997; Fig. 3). This southern strand, which is associated with fault scarps developed on Pleistocene fan deposits (unit Qf1), likely continues southwestward into the Rito Cieneguilla valley, where it may be the primary strand of the Embudo fault. The northern and middle strands cross NM-68 at roadcuts 1 and 2, respectively (Figure 3; Muehlberger, 1979). These two strands merge into a single strand southwest of Arroyo Hondo (Fig. 3).

The northern fault strand is associated with a prominent, 12-m-high north-facing scarp developed on early Pleistocene fan deposits (unit Qf1) (Machette and Personius, 1984). As exposed in roadcut 1, the northern strand is a low-angle reverse fault along which sand and gravel of the Miocene Ojo Caliente Member of the Tesuque Formation is thrust-faulted over Qf1 deposits (Muehlberger, 1979). About 200 m east of NM-68, the northern strand of the Embudo fault is marked by a 1.5-m-high scarp on latest Pleistocene to Holocene fan deposits, and a small left-deflection in an unnamed arroyo (Kelson et al., 1997a).

The middle fault strand exposed in roadcut 2 (Fig. 3) is associated with strongly tilted and folded strata of the late Tertiary Santa Fe Group (Muehlberger, 1979). As sketched by Muehlberger (1979), the exposure shows a low-angle, north-vergent secondary thrust fault that dips about 30˚ southeast, and displaces beds within the Miocene Chama-El Rito Member of the Tesuque Formation. This secondary fault is dramatic in the exposure, but has less than 2 m of total stratigraphic separation. The amount of separation on this fault gradually decreases upward, with little or no discernible separation at the northern end of the roadcut. The primary 2-m-wide fault zone exposed in roadcut 2 is located southeast of the secondary thrust fault, and was not sketched by Muehlberger (1979). The primary fault dips moderately (50˚) southeast and has a minimum stratigraphic separation of 4 m of Chama-El Rito Member sediment. Kinematic indicators on the primary fault include sigmoidal “s” shears in the fault zone and moderately plunging slickensides (15˚ toward S65˚W, with a rake of less than 10˚). Collectively, these relations suggest left-lateral slip on the fault zone. On the opposite (western) side of the highway, the roadcut exposes only a single, steeply northwest-dipping fault that juxtaposes distinct facies of the Santa Fe Group strata. This fault dips steeply northwest, and has grooves

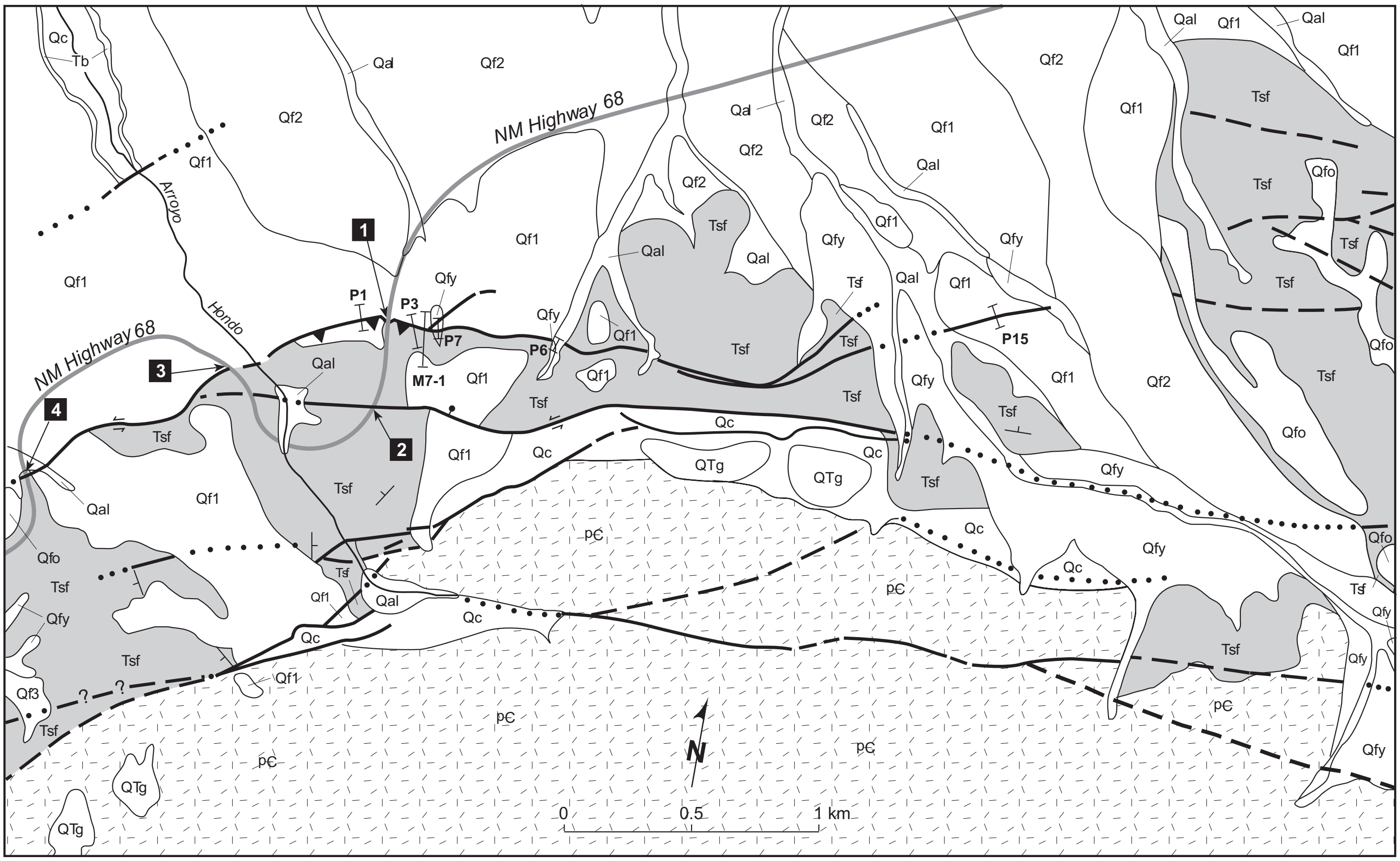

Explanation

Qal Stream channel and valley-floor alluvium, and active floodplains (Holocene).

Qe Eolian sand sheets and dunes (late Pleistocene to Holocene).

Qls Landslide deposits (late Pleistocene to Holocene).

Qc Colluvium (middle Pleistocene to Holocene).

Qfy Alluvial-fan deposits (late Pleistocene to Holocene).

Qf3 Alluvial-fan deposits (middle to Late Pleistocene).

Qf2 Alluvial-fan deposits (middle Pleistocene).

Qf1 Alluvial-fan deposits (early Pleistocene), contains ash dated at 1.27 ± 0.02 Ma (W. McIntosh, personal communication, 1996).

Qtrg Fluvial gravel deposited by ancestral Rio Grande (early to middle Pleistocene).

QTg Coarse-grained alluvial-fan(?) deposit preserved as thin gravel remnants (Pliocene? to early Pleistocene?).

Tb Servilleta Basalt, undifferentiated (Pliocene).

Tsf Santa Fe Group sediments, undifferentiated (Tertiary).

pC̶ Undifferentiated bedrock, including quartzite, slate, amphibolite, gneiss, and other metamorphic rocks (Precambrian).

Map Symbols

Contact, dashed where uncertain, dotted where buried.

Fault, dashed where uncertain, dotted where buried; ball on downthrown side, barbs on thrust plate.

Strike and dip direction of bedding.

Landslide, arrows show direction of movement.

2 Roadcut exposure (Muehlberger, 1979).

P1 Topographic profile

Anticline in Servilleta basalt

Syncline in Servilleta basalt

FIGURE 3. Surficial geologic map along the Embudo fault near Arroyo Hondo (after Bauer and Kelson, 1999).

and mullions on the fault plane that plunge 20˚ to 23˚ southwest. These relations also suggest left-normal oblique slip along the primary strand of the Embudo fault. The prominent low-angle thrust exposed in roadcut 2 likely is a minor reverse splay of the primary left-lateral fault strand, and suggests the presence of a local positive flower structure along the fault.

Thus, roadcut exposures of the Embudo fault near Arroyo Hondo show that the main fault strand is moderately to steeply dipping and has had predominantly left-lateral slip. These geometric relations and kinematic interpretations differ substantially from previously published interpretations of the Embudo fault based on the same exposures (Muehlberger, 1979). We infer that the south-dipping reverse faults identified by Muehlbeger (1979) are secondary structures that splay upward from the primary left-lateral shear zone in the shallow subsurface, and form a positive flower structure. The thrust faults probably are a geometric result of a right step in the fault (Fig. 2), which is consistent with interpretations of local shortening within restraining step-overs elsewhere along the fault (Steinpress, 1981; Hall, 1988).

Reach D (Pilar Mesa and Rito Cieneguilla Valley)

This 5-km-long reach extends from the Arroyo Hondo area southwest to the Rio Grande near the town of Pilar, in the vicinity of Pilar Mesa (Fig. 2). This mesa is underlain by Miocene sediments of the Santa Fe Group, Pliocene Servilleta Basalt, and Quaternary surficial deposits (Figure 4). The N60˚E strike of the fault along this reach is the same as the regional strike of the

Embudo fault across the Rio Grande rift between Pilar and Clara Peak (Fig. 1). Reach D includes a southern fault strand located within the deeply dissected Rito Cieneguilla valley between Pilar Mesa and the Picuris Mountains, and a northern fault strand along the top of Pilar Mesa. Within the Rito Cieneguilla valley, the southern fault strand is poorly located and either merges with the "Border fault" of Leininger (1982) along the eastern margin of the Rito Cieneguilla valley, or extends through the central part of Rito Cieneguilla beneath young alluvial valley-fill deposits. In either scenario, the southern fault strand probably merges with the Proterozoic Pilar shear zone at the southern end of the Rito Cieneguilla valley (Bauer and Helper, 1994; Kelson and Bauer, 1998).

The northern strand of the Embudo fault along Pilar Mesa is well expressed by northwest-facing scarps on early Pleistocene ancestral Rio Grande deposits (unit Qtrg) and alluvial-fan deposits (unit Qfo) (Kelson et al., 1997a; Fig. 4). However, the scarps on these deposits are substantially lower than those on the same deposits on reach C near Arroyo Hondo to the northeast. For example, there is no displacement of early Pleistocene fan deposits (unit Qf1) along reach D, although there is as much as 12 m of northwest-down NVTD near Arroyo Hondo, just 3.5 km to the northeast. Also, the vertical separation decreases to the southwest along Pilar Mesa; for example, early Pleistocene deposits (unit Qfo) are displaced 5 m at the northeastern end of reach D, but have only 2.5 m of northwest-down NVTD in the central part of the mesa. At the southwestern end of the mesa (Fig. 4), the Pliocene Servilleta Basalt has only about 3.5 m of northwest-down NVTD.

Previous workers stated that the sense of vertical separation on the Embudo fault changes at a point about 2 km northeast of Pilar (Muehlberger, 1979; Leininger, 1982; Dungan et al., 1984). This interpretation is based, in part, on a northwest-facing fault scarp and northwest-down separation of the Servilleta Basalt in the central and northern parts of the mesa, and a southeast-facing topographic scarp on the southern part of the mesa. However, recent mapping provides evidence of northwest-down fault displacement along the entire mesa (Fig. 4), and thus argues against a hinge point along the fault on Pilar Mesa (Kelson and Bauer, 1998). The northern strand of the Embudo fault at the southern tip of Pilar Mesa is not associated with a southeast-facing fault scarp (Leininger, 1982). Instead, recent mapping demonstrates the presence of northwest-down displacement of the Servilleta Basalt and overlying Rio Grande gravel (unit Qtrg) at the southern end of Pilar Mesa (Kelson and Bauer, 1998; Fig. 5). There is about 3.5 m of net northwest-down displacement of the base of the Qtrg gravel (Fig. 5). Although there are several landslides at the southern end of the mesa that involve the gravel, Servil-

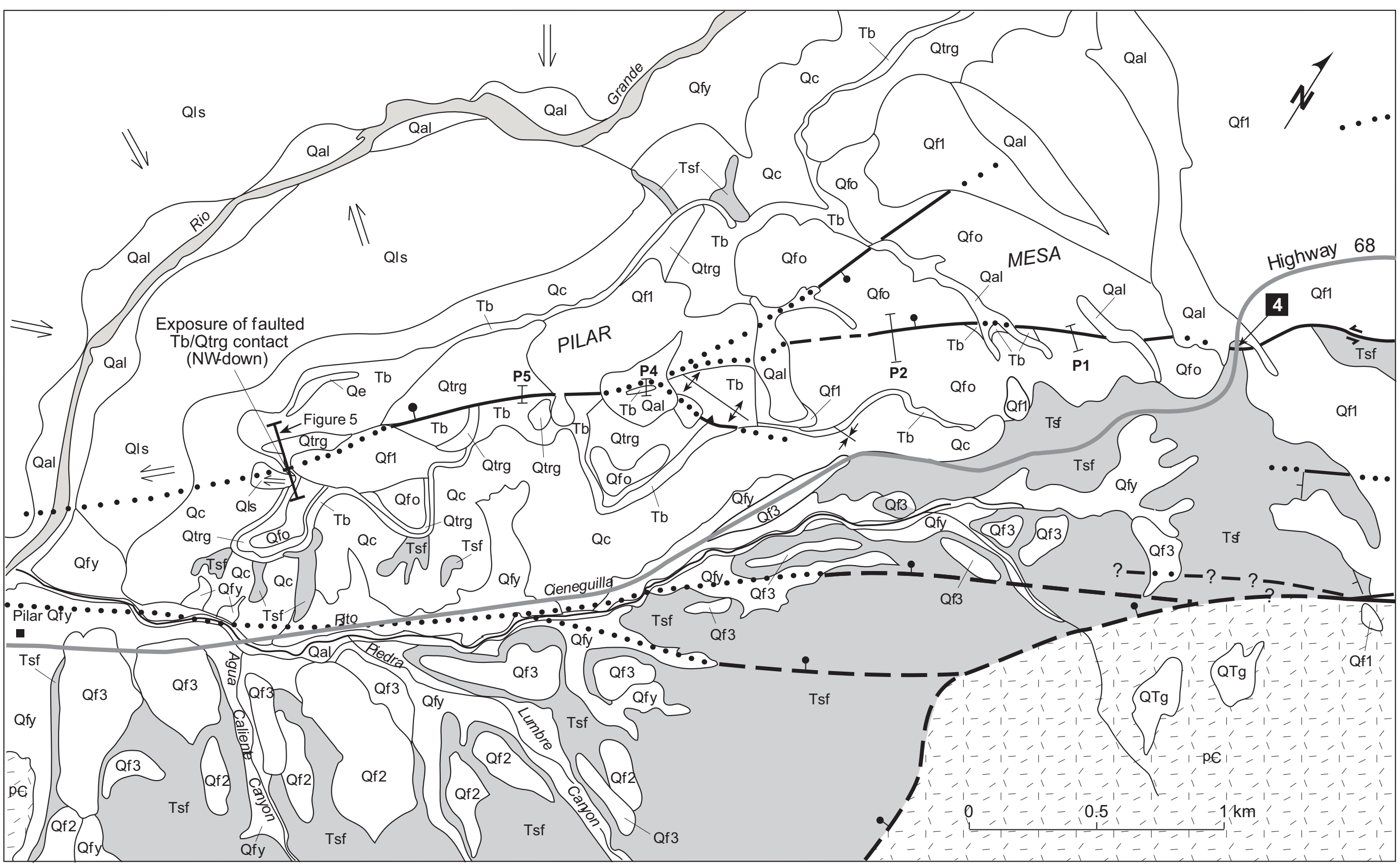

FIGURE 4. Surficial geologic map along the Embudo fault between Pilar and Arroyo Hondo (after Kelson and Bauer, 1998; Bauer and Kelson, 1997). Description of map units and symbols shown on Figure 3.

leta Basalt, and underlying Tesuque Formation, detailed mapping demonstrates that the northwest-down displacement is unrelated to landsliding. The lowermost flow unit of the Servilleta Basalt is continuous across the southern end of Pilar Mesa, with the exception of the 3.5 m northwest-down displacement at the Embudo fault (Fig. 5).

Muehlberger (1979), Leininger (1982), and Dungan et al. (1984) all argued that the presence of one flow unit on the east side of the fault and multiple flow units on the western side is related to east-down displacement. These relations, and the continuity of the lowermost flow unit beneath the southeast-facing topographic scarp, instead are best explained by erosion of upper flow units by the ancestral Rio Grande during Qtrg time. Incision of the ancestral river into the basalt removed the uppermost flow units, and the ancestral channel was filled with a thick (up to 30 m) section of gravel (unit Qtrg) above the remaining lowermost flow unit. Thus, our mapping (Kelson and Bauer, 1998) does not support the interpretation of a southeast-down fault by previous workers on the basis of the number of flow units. Our observations and interpretations of the geomorphic history of Pilar Mesa lead to the conclusion that the northern strand of the Embudo fault near Pilar Mesa has had northwest-down displacement. The relatively small amount of post-Pliocene displacement also suggests that the northern fault strand on Pilar Mesa is not the primary strand of the Embudo fault in this area. The primary fault strand probably lies within the dissected Rito Cieneguilla valley (Fig. 4).

Summary of Late Quaternary Faulting

Detailed field mapping and topographic profiling shows that there is considerable variation in the geomorphic expression of the northeastern 18 km of the Embudo fault between Pilar and Talpa. Much of this variation is a result of differences in the ages

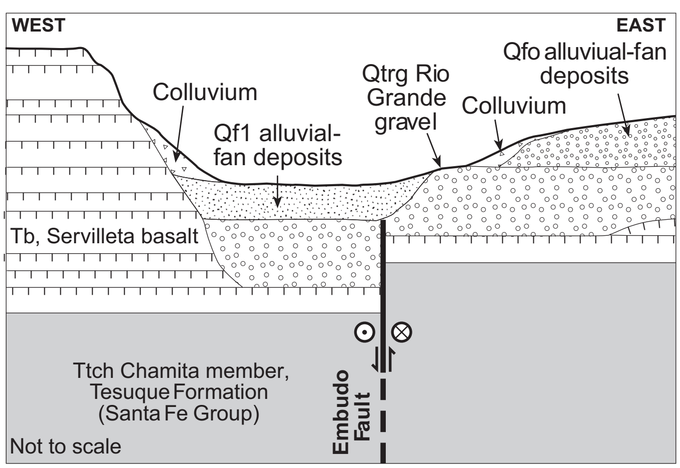

FIGURE 5. Schematic geologic cross section across the southern end of Pilar Mesa, showing relationships between east-facing topographic scarp along the western margin of the early Pleistocene Rio Grande gravel (unit Qtrg) and the location of the west-down northern strand of the Embudo fault along reach D. The 3 Ma Servilleta Basalt has about 3.5 m of northwest-down vertical separation across this fault strand.

of surficial deposits that the fault crosses, as well as differences in the amounts of vertical separations along the fault length (Fig. 6). However, scarp heights on similar-aged deposits vary substantially along the fault, and there are no obvious relations among scarp height, age of faulted deposit, and location along the fault (Kelson et al., 1997a). However, strike-slip faults commonly have substantial variations in vertical separation along strike, including reversals in the sense of separation over short distances. In addition, lateral- or oblique-slip may produce abrupt differences in scarp heights along the fault, depending on the amount of local topographic relief and the net slip vector. Given that the Embudo fault has had predominantly left-normal slip, substantial variations in separation along the fault may be expected.

The variable scarp heights along the fault appear to be correlated with different fault reaches. For example, the north-down NVTD of the early Pleistocene Qf1 alluvial-fan deposits is relatively high (8 to 10 m) along reach A, low (1.6 m) along reach B, and very high (12 m) along reach C (Fig. 6). This deposit has no vertical separation on Pilar Mesa (reach D). Using the NVTD of this deposit as a guide, we interpret that similar variations are present in other surficial deposits along the fault (Fig. 6). This assumes that the variations in scarp height along the fault have been persistent through the late Quaternary.

We interpret that these variations reflect, in a large part, differences in the relative amounts of lateral and vertical displacement along the fault, which in turn may be related to the local strike of the fault relative to the direction of regional extension (Fig. 7). Assuming a rift extension direction of due west, geometry suggests that the N60˚E-striking reach A would exhibit a ratio between left-lateral and fault-normal slip of about 2:1 (Fig. 7). The east-striking reach B is nearly parallel to the presumed extension direction, and probably has a ratio of about 10:1 or greater. Reach C exhibits structural evidence of local shortening and reverse faulting, and appears to be a right-restraining bend or step-over between reaches B and D. The prominent scarp along this reach therefore is related to local fault interactions and/or a restraining bend. We do not estimate a ratio between lateral and vertical slip components along reach C because of this local-scale deformation. Reach D, in turn, has a northeast strike similar to reach A (Fig. 7), and probably has a ratio between lateral and vertical slip components of about 2:1.

These expected ratios are consistent with the distribution of vertical separation along the fault, as shown in Fig. 6, and with the pattern and geomorphic expression of faulting along the fault. Along reach A, the moderately high scarps, relatively simple fault map pattern, and northwest-down displacements are consistent with left-normal (about 2:1) slip. Reach B, in contrast, has low scarps, a broad, complex fault pattern with multiple anastomosing fault strands, and both north-down and south-down displacements. These relations appear to be related to a large component (about 10:1) of lateral slip. Reach C is characterized by relatively high fault scarps along reverse faults, and a complex fault pattern consistent with a positive flower structure within a restraining step-over. Lastly, reach D exhibits moderate to low fault scarps, a relatively simple, linear fault trace, and northwest-down displacements consistent with left-normal slip. Thus, the geo-

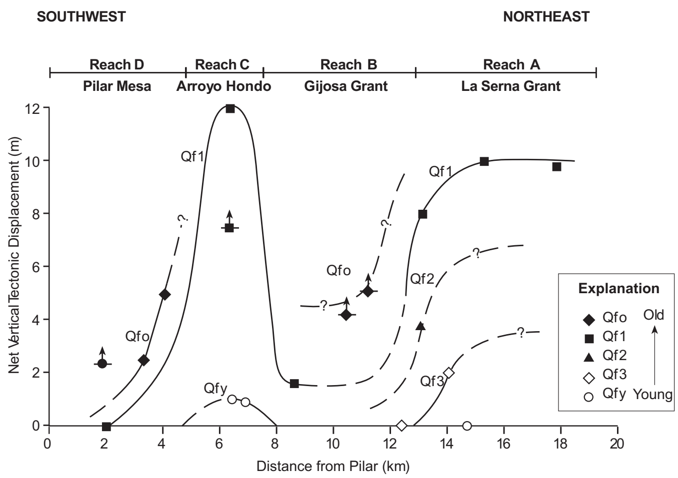

FIGURE 6. Net vertical tectonic displacement along the Embudo fault between Pilar and Talpa. Data based on topographic profiles of fault scarps across surficial deposits, and interpretation based on local fault reaches. Arrows on data points indicated minimum values

morphic expression of the Embudo fault is strongly influenced by local fault strike with respect to the predominant east-west regional extension direction.

TIMING OF LATE QUATERNARY DEFORMATION

Detailed mapping along the northeastern 18 km of the Embudo fault provides a means to qualitatively estimate the age of late Quaternary surface ruptures. At several localities along the fault, scarps developed on higher, older geomophic surfaces exhibit greater displacement than younger, inset surfaces. The higher scarps generally exhibit bevels, which also suggest that multiple surface ruptures have occurred along the fault. The youngest map unit displaced by the Embudo fault is the latest Pleistocene to Holocene (≤30 ka) alluvial-fan deposit (unit Qfy, Bauer et al., 1999), although faulting of this deposit is identified only within the Arroyo Hondo area (reach C; Figure 2). At both of the localities where these young fans cross a fault strand in this restraining step-over, there are subtle scarps as much as 1.5 m high that reflect about 1.0 m of northwest-down NVTD. This provides evidence that the fault, at least locally, has had surface rupture during the latest Pleistocene to Holocene. Along reach B (Fig. 2), these young fan deposits show no prominent evidence of vertical displacement, although we cannot preclude the possibility of small amounts of late Quaternary lateral slip or broadly distributed surface deformation along this reach. Small fans mapped as unit Qfy east of Arroyo del Alamo (in reach A) do not have prominent fault scarps, although air-photo lineaments are present that may be related to surface faulting. In summary, our mapping suggests possible latest Pleistocene to Holocene surface rupture along the Arroyo Hondo restraining step-over (reach C, Fig. 2), and possible rupture within the past 30 ka or so along reaches A and B of the northeastern section of the Embudo fault. The timing of ruptures along reach D is not known, primarily because of lack of continuous geomorphic surfaces within the dissected Rito Cieneguilla valley.

FAULT SEGMENTATION AND CONTINUITY OF RUPTURES

Field relations support a fault segment boundary between the southern Sangre de Cristo and northeastern Embudo faults at the change in orientation of the Sangre de Cristo Mountains range front near the village of Talpa (Menges, 1988, 1990; Machette et al., 1998). The southern Sangre de Cristo fault has prominent latest Pleistocene fault scarps exhibiting west-down displacement (Machette and Personious, 1984; Kelson et al., 2004, this volume). Overall, the fault scarps on late Quaternary surficial deposits are continuous and lie within a zone less than 2 km wide (Machette and Personious, 1984; Menges, 1988, 1990; Bauer et al., 2001). In comparison, the northeastern section of the Embudo fault is characterized by a much less continuous series of fault strands. Prominent fault scarps are present only at a few localities, and overall the fault is characterized by a distributed pattern of discontinuous scarps and lineaments. Considering that both the Embudo and Sangre de Cristo faults exhibit evidence of late Pleistocene rupture (Kelson et al., 2004, this volume; Machette et al., 1998), the difference in map pattern may be related to differing styles of deformation. The discontinuous pattern of rupture along the northeastern Embudo fault likely is related to left-lateral displacement, with localized uplift along the restraining step-over near Arroyo Hondo. These relations support the interpretation that the northern boundary of the northeastern Embudo fault is near the village of Talpa (Machette and Personious, 1984; Machette et al., 1998). We concur with previous interpretations that the southern boundary of the section is near the village of Embudo, on the basis of a reversal in the sense of vertical separation between the west-down San Luis Basin and the east-down Española Basin (Machette et al., 1998).

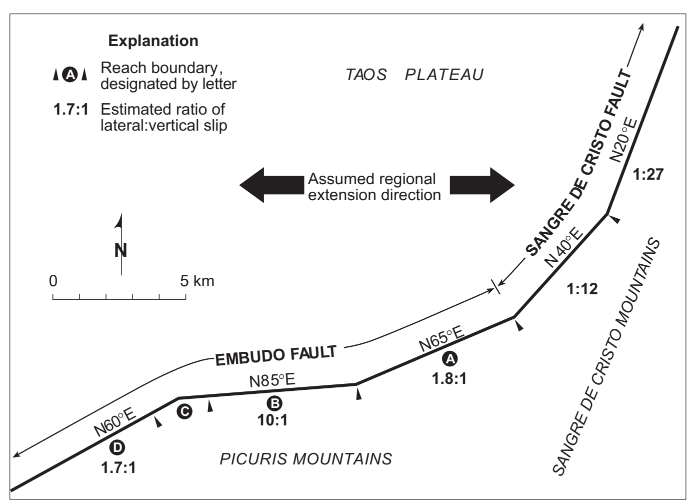

FIGURE 7. Schematic diagram of the Embudo and Sangre de Cristo faults, showing local fault reaches, assumed east-west regional extension direction, and calculated ratios between lateral and vertical components of slip based on fault strike.

APPLICATION TO REGIONAL TECTONIC INTERPRETATIONS OF THE NORTHERN RIO GRANDE RIFT

The Rio Grande rift in northern New Mexico and southern Colorado is composed of a series of north-trending, elongate topographic and structural basins (San Luis, Española, Santo Domingo, and Albuquerque basins). In general, these basins are broad half grabens that are tilted either to the east or west, and are bordered on one margin by a relatively active, north-striking rift-border fault. These basins are arranged in a right-stepping *en echelon* pattern, and likely are separated by northeast-trending transfer fault zones that accommodate the differential sense of basin tilting (Lozinsky, 1994; Russell and Snelson, 1994; Chapin and Cather, 1994).

The Embudo fault extends across the Rio Grande rift from the Pajarito fault near Los Alamos, to the Sangre de Cristo fault near Taos (Kelley, 1978; Muehlberger, 1979; Aldrich and Dethier, 1990; Gonzalez and Dethier, 1991; Wong et al., 1996; Fig. 1). Previous workers have identified reversals in the sense of vertical separation along the fault, with most workers agreeing that the location of the possible hinge point lies approximately in the central part of the fault near Embudo (Kelley, 1978; Muehlberger, 1979; Personius and Machette, 1984; Ferguson et al., 1995; Machette et al., 1998). Overall, the geometry of the Embudo fault, and its relationship to the Española and San Luis Basins, is similar to accommodation zones in other continental rift systems (Rosendahl, 1987; Faulds and Varga, 1998).

However, some previous studies suggest that the kinematics of deformation along the Embudo fault may be more complicated than suggested by the simple model that the fault is a rift transfer zone. Local thrust faulting along the northern part of the Embudo fault near Arroyo Hondo led Muehlberger (1979) to postulate that the fault locally accommodates north-south crustal shortening rather than differential crustal extension. In turn, this led to the suggestion that the Española Basin, and the adjacent southern Sangre de Cristo Mountains between Taos and Santa Fe, have undergone counterclockwise rotation driven by oblique rift extension (Muehlberger, 1979; Aldrich, 1986; Brown and Golombek, 1986). This model interprets movement on the Embudo fault as north-vergent thrust faulting of the Picuris Mountains over the San Luis Basin. Thus, although the roadcut exposures of the Embudo fault near Arroyo Hondo represent only a small glimpse of the structural character of the fault, they have previously played a critical role in the tectonic interpretation of the entire northern Rio Grande rift.

This previous tectonic model, however, is called into question on the basis of recent paleomagnetic data, regional fault-activity assessments, and our re-interpretation of the Arroyo Hondo roadcut exposures. First, field studies by Salyards et al. (1994) provide data that argue against large-scale rotation of the Española Basin. Paleomagnetic data throughout the basin show non-uniform rotations, with greater amounts of rotation near basin-bounding faults (Salyards and Ni, 1990; Salyards et al., 1994). Second, active rotation of a structural block that includes the entire Española Basin and southern Sangre de Cristo Mountains requires similar rates and activities of the faults bounding this domain, including the Embudo, Pajarito, La Bajada, San Francisco, Tijeras, and Picuris-Pecos faults. However, regional assessments of fault activity (Kelson and Olig, 1995; Wong et al., 1996; Machette et al., 1998) suggest that the activities and senses of slip along faults bordering the Española Basin and southern Sangre de Cristo Mountains are inconsistent with regional rotation. For example, the Pajarito fault, which borders the western margin of the Española Basin, is dominated by east-down normal displacement rather than lateral slip (Wong et al., 1996; Olig et al., 1996). Also, the Picuris-Pecos fault shows no evidence of late Quaternary activity (Machette et al., 1998) that would be expected if the Española Basin and the southern Sangre de Cristo Mountains were rotating as a structural block. Lastly, as a whole, there is an order of magnitude difference in the slip rates along faults along which the rotation should occur (Kelson and Olig, 1995).

Lastly, our investigation provides additional evidence that left-normal oblique slip, rather than north-directed thrust faulting (as previously postulated), characterizes the northeastern part of the Embudo fault. We believe that the thrust faults in the Arroyo Hondo roadcut exposures sketched by Muehlberger (1979, Fig. 2) are, in fact, secondary features related to a restraining step-over within a left-lateral fault zone, rather than to northward thrusting of the Picuris Mountains over the Taos Plateau. Our detailed mapping of the Embudo fault and associated kinematic data do not support the hypothesis that the Embudo fault presently is associated with counterclockwise rotation of the Española Basin. Instead, the northeastern section of the Embudo fault more likely accommodates regional extension through left-normal oblique slip, as might be expected for a northeast-striking transfer zone that traverses the northern Rio Grande rift. This is consistent with accommodation of east-west rift-normal extension in both the San Luis and Española basins.

APPLICATION TO SEISMIC HAZARD ASSESSMENT IN THE NORTHERN RIO GRANDE RIFT

In general, the seismic potential of transfer fault zones is poorly understood, with no known historical examples of surface rupturing earthquakes and no documented examples of paleoearthquakes along structures that trend obliquely across active rifts. However, in order to evaluate seismic hazard in the northern Rio Grande rift, the Embudo fault must be characterized. Thus we consider two end-member scenarios for the seismic potential of the northeastern Embudo fault:

(1) Surface rupture on the Embudo fault occurs as sympathetic slip only during coseismic slip on either of the adjacent major basin-bounding faults (i.e., the Pajarito or Sangre de Cristo faults). The fault thus serves primarily to accommodate differential subsidence at the margins of the San Luis and Española Basins. In this scenario, the Embudo fault is a “passive” structure that does not independently accumulate significant elastic strain. Instead of being a source for moderate or large earthquakes, the fault forms a structural termination or rupture barrier for the major basin-bounding faults. This is supported by the absence of

instrumental seismicity clearly associated with the Embudo fault (House and Hartse, 1995).

(2) The Embudo fault may be an “active” seismic source that accumulates strain and releases it during moderate to large earthquakes. In this scenario, earthquakes occur on the Embudo fault independent of surface-rupturing earthquakes on the major basin-bounding faults to the north and south.

Because the late Quaternary earthquake history along the Embudo fault is still unknown, evidence of late Quaternary displacement warrants that it be considered conservatively as an independent seismogenic source (Kelson et al., 1997b). Machette et al. (1998) identified two fault sections based on differences in geomorphic expression and sense of vertical separation. The 35-km-long northeastern section of the fault was identified as extending from a possible hinge point near the town of Embudo (Machette and Personius, 1984) to an intersection with the Sangre de Cristo fault near Ranchos de Taos. The southwestern section of the fault was assumed to extend about 30 km from Clara Peak on the south to Embudo (Machette et al., 1998). Wong et al. (1996) considered rupture scenarios in which: (1) each of these sections ruptures independently during **M**6.8 (moment magnitude) earthquakes; (2) the two fault sections rupture together during a larger, **M**7.3 earthquake. Because of considerable structural complexities along the fault, and the reversal in sense of vertical separation near the town of Embudo, it seems unlikely that the entire Embudo fault would rupture during a single, large-magnitude earthquake. Other possible scenarios include rupture along sections of the Embudo fault with rupture on adjacent rift-margin faults (i.e., the Pajarito or Sangre de Cristo faults). We believe that the most realistic rupture scenarios, given the available data, are individual ruptures on either the northeastern or the southwestern fault sections. Thus, based on empirical relationships between rupture length and magnitude (Wells and Coppersmith, 1994), we interpret that, as independent seismic sources, the maximum (moment) magnitude for the 35-km-long northeastern Embudo fault is **M**6.9, and for the 30-km-long southwestern Embudo fault is **M**6.8.

CONCLUSIONS

The 65-km-long northeast-striking Embudo fault is a major structural feature that has played an important role in the late Cenozoic deformation of the actively extending Rio Grande rift. This fault forms the structural boundary between the east-tilted San Luis Basin on the north and the west-tilted Española Basin on the south, both of which are bordered by major normal faults showing late Pleistocene to Holocene surface ruptures. This investigation concentrated on assessing the pattern, timing, and kinematics of Quaternary deformation along the northeastern 18 km of the Embudo fault between the villages of Pilar and Talpa, where the fault borders the Taos Plateau and has locally prominent geomorphic expression on late Quaternary deposits.

Surficial deposits along the northeastern 18 km of the Embudo fault consist primarily of alluvial fans shed to the north from the Picuris Mountains into the southern San Luis Basin. The fans range in age from early Pleistocene to Holocene, and provide a series of long-term indicators of the style and amounts of Quaternary fault displacement. The northeastern part of the Embudo fault exhibits a complex pattern of late Quaternary deformation, along four short reaches that range in length from 2 to 7 km. These reaches probably reflect variations in the style of near-surface deformation that appear to be related to the local sense of slip and fault complexities. In general, the eastern reach A has a few continuous fault strands, relatively high fault scarps, and west-down left-normal oblique slip. Reach B, in contrast, has poor geomorphic expression, low fault scarps across older fan deposits, and many very discontinuous fault strands within a broad zone of faulting. The 2-km-long reach C has continuous fault strands, relatively high fault scarps on reverse faults, and is a restraining step-over between reaches B and D. The western reach D contains a northern fault strand along Pilar Mesa that has geomorphic expression and northwest-down vertical displacement decreasing from north to south, and a southern fault strand that is poorly expressed within the dissected Rito Cieneguilla valley.

Detailed field mapping in the Arroyo Hondo area (reach C) has led us to revise a previous interpretation of roadcuts exposing the Embudo fault (Muehlberger, 1979). Kinematic indicators in the roadcut exposures suggest that the fault has a component of left-lateral slip. Thrust faults previously mapped by Muehlberger (1979) splay upward from a high-angle left-lateral shear zone, and form a positive flower structure. We infer that the thrust faults are secondary features related to a right step-over in the fault, and that the principal strand of the northeastern Embudo fault is a steeply dipping to vertical left-normal oblique fault. Because these roadcuts formed a primary basis for interpretations that the entire Española Basin has rotated counterclockwise, our interpretation that the thrust faults are related to a local restraining step-over argues against the block-rotation model. Thus, we believe that the data developed in this study provides evidence against significant northward thrusting of the Picuris Mountains over the southern San Luis Basin, as postulated by Muehlberger (1979).

As might be expected along a complex, oblique-slip fault, the geomorphic expression and pattern of late Quaternary faulting are directly related to the local strike of the fault relative to the east-west orientation of regional extension. We interpret that the local sense of net slip varies substantially along the Embudo fault between Pilar and Talpa, with local reaches exhibiting left-normal, left-lateral, and reverse displacements. Geomorphic expression along the fault is most prominent where faults have a substantial component of vertical slip, particularly where reverse displacement has occurred within a local restraining step-over between reaches having left-lateral or left-normal slip. These relations highlight the need for an understanding of local fault kinematics in order to adequately assess fault slip rates.

Our detailed surficial mapping suggests the occurrence of latest Pleistocene to Holocene surface deformation along the northeastern section of the Embudo fault. However, evidence of this young deformation is prominent only within the 2-km-long restraining step-over near Arroyo Hondo, and there is poor geomorphic expression of young faulting along other, adjacent reaches of the fault. Because of the large component of lateral slip along the fault and consequent poor geomorphic expression along some fault reaches, we interpret that the most-recent surface deformation also extended along most, if not all, of the 18-km-long part of the fault between Pilar and Talpa. Because of considerable structural complexities along the fault and the reversal in the sense of vertical separation near the town of Embudo, it seems unlikely that the entire 65-km-long Embudo fault would rupture during a single, large-magnitude earthquake. We believe that the most realistic rupture scenarios are individual ruptures on either the 35-km-long northeastern fault section or the 30-km-long southwestern fault section. The maximum (moment) magnitude earthquakes for these scenarios are estimated to be **M**6.9 and **M**6.8, respectively.

ACKNOWLEDGMENTS

This research was supported, in part, by the U.S. Geological Survey (USGS), Department of the Interior, under USGS award number 1434-96-G-02739. The views and conclusions contained in this document are those of the authors and should not be interpreted as necessarily representing the official policies, either expressed or implied, of the U.S. Government. Some of this research also was completed for the New Mexico Bureau of Geology and Mineral Resources STATEMAP program, and partial funding was provided by William Lettis & Associates, Inc. Thanks to Michael Machette (USGS) for providing encouragement during the study and scarp profile data from the Embudo and Sangre de Cristo faults. Thanks also to Jamie Gardner (Los Alamos National Laboratory), Michael Machette, and William Lettis for technical reviews that helped clarify this manuscript.

REFERENCES

Aldrich, M.J., Jr., and Dethier, D.P., 1990, Stratigraphic and tectonic evolution of the northern Española basin, Rio Grande rift, New Mexico: Geological Society of America Bulletin, v. 102, p. 1695-1705.

Bauer, P.W., 1988, Precambrian geology of the Picuris Range, north-central New Mexico [Ph.D. dissertation]: New Mexico Bureau of Geology and Mineral Resources Open-file Report OF-325, 280 p.

Bauer, P.W., and Helper, M., 1994, Geology of the Trampas quadrangle, Taos County, NM: New Mexico Bureau of Geology and Mineral Resources Open-file Map OF-GM 71, scale 1:24,000.

Bauer, P.W., and Kelson, K.I., 1997, Geology of the Taos SW quadrangle, Taos County, NM: New Mexico Bureau of Geology and Mineral Resources Open-file Map OF-GM 12, scale 1:24,000.

Bauer, P.W. and Kelson, K.I., 2001, Geology of the Taos 7.5-minute quadrangle, Taos County, New Mexico: New Mexico Bureau of Geology and Mineral Resources, Open-file Geologic Map OF-GM 43, scale 1:24,000.

Bauer, P.W., Kelson, K.I., Lyman, J., Heynekamp, M.R., and McCraw, D.J., 1999, Geology of the Ranchos de Taos quadrangle, Taos County, NM: New Mexico Bureau of Geology and Mineral Resources Open-file Map OF-GM 33, scale 1:24,000.

Bradford, S.C., 1992, Kinematics of an accommodation zone in the Rio Grande rift; the Embudo fault zone, northern New Mexico: [M.S. thesis]: Ohio State University, 177 p.

Brown, L.L. and Golombek, M.P., 1985, Tectonic rotations within the Rio Grande rift - Evidence from paleomagnetic studies: Journal of Geophysical Research, v. 90, no. B1, p. 790-802.

Chapin, C. E., and Cather, S. M., 1994, Tectonic setting of the axial basins of the northern and central Rio Grande rift: Geological Society of America Special Paper 291, p. 5-25.

Dungan, M.A., Muehlberger, W.R., Leininger, L. Peterson, C., McMillan, N.J., Gunn, G., Lindstrom, M., and Haskin, L., 1984, Volcanic and sedimentary stratigraphy of the Rio Grande Gorge and late Cenozoic geologic evolution of the southern San Luis Valley: New Mexico Geological Society, 35th Field Conference, Guidebook, p. 157-170.

Faulds, J. E. and Varga, R. J., 1998, The role of accommodation zones and transfer zones in the regional segmentation of extended terranes: *in* Faulds, J. E. and Stewart, J. H., eds., Accommodation Zones and Transfer Zones: The Regional Segmentation of the Basin and Range Province: Geological Society of America, Special Paper 323, p. 1-45.

Ferguson, J.F., Baldridge, W.S., Braile, L.W., Biehler, S., Gilpin, B., and Jiracek, G.R., 1995, Structure of the Española basin, Rio Grande rift, New Mexico, from SAGE seismic and gravity data: New Mexico Geological Society, 46th Field Conference, Guidebook, p. 105-110.

Gonzalez, M.A., and Dethier, D.P., 1991, Geomorphic and tectonic evolution along the margin of the Colorado Plateau and Rio Grande rift, northern New Mexico: New Mexico Bureau of Geology and Mineral Resources Bulletin 137, p. 29-45.

Gardner, J.N., and House, L., 1987, Seismic hazards investigations at Los Alamos National Laboratory, 1984 to 1985: Los Alamos National Laboratory Report LA-11072-MS, 76 p.

Gardner, J.N., Reneau, S.L., Lavine, A., Lewis, C.J., Katzman, D., McDonald, E.V., Lepper, K., Kelson, K.I., and Wilson, C., 2003, Paleoseismic trenching in the Guaje Mountain fault zone, Pajarito fault system, Rio Grande rift, New Mexico: Los Alamos National Laboratory Report LA-14087-MS, 68 p.

Hall, M.S., 1988, Oblique slip faults in the northwestern Picuris Mountains of New Mexico; an expansion of the Embudo transform zone: [M.S. thesis: University of Texas at Austin, 69 p.

Hillman, D.M., 1986, A study of small-scale deformation features associated with the Embudo fault zone, north-central New Mexico: unpublished M.S. thesis, The University of Oklahoma, Tulsa, 83 p.

House, L., and Hartse, H., 1995, Seismicity and faults in northern New Mexico: New Mexico Geological Society, 46th Field Conference, Guidebook, p. 135-137.

Kelley, V.C., 1978, Geology of the Española Basin, New Mexico: New Mexico Bureau of Mines & Mineral Resources Geologic Map 48, scale 1:125,000.

Kelson, K.I., and Bauer, P.W., 1998, Geology of the Carson quadrangle, Taos County, New Mexico: New Mexico Bureau of Geology and Mineral Resources Open-file Map OF-GM 22, scale 1:24,000.

Kelson, K.I., and Bauer, P.W., 2003, Geology of the Los Cordovas quadrangle, Taos County, New Mexico: New Mexico Bureau of Geology and Mineral Resources Open-file Map OF-GM 63, scale 1:24,000.

Kelson, K. I., and Olig, S.S., 1995, Estimated rates of Quaternary crustal extension in the Rio Grande rift, northern New Mexico: New Mexico Geological Society, 46th Field Conference, Guidebook, p. 9-12.

Kelson, K. I., Unruh, J.R., and Bott, J.D.J., 1997a, Field characterization, kinematic analysis, and initial paleoseismologic assessment of the Embudo fault, northern New Mexico: Final Technical Report, USGS Award 1434-96-G-02739, 48 p.

Kelson, K. I., Unruh, J.R., Bott, J.D.J., and Bauer, P.W., 1997b, Paleoseismology of accommodation zones in an active rift: Interpretations of the Embudo fault, Rio Grande rift, New Mexico: Geological Society of America Abstracts with Programs, p. A-72.

Kelson, K.I., Bauer, P.W., Connell, S.D., Love, D., Rawling, G., and Mansell, M. 2004b, Initial paleoseismic and hydrogeologic assessment of the southern Sangre de Cristo fault at the Taos Pueblo site, Taos County, New Mexico: New Mexico Geological Society, 55th Field Conference, Guidebook, p.289-299.

Leininger, R.L., 1982, Cenozoic evolution of the southernmost Taos plateau, New Mexico: [M.S. thesis]: Universtiy of Texas at Austin, 110 p.

Lozinsky, R.P., 1994, Cenozoic stratigraphy, sandstone petrology, and depositional history of the Albuquerque Basin, central New Mexico: Geological Society of America Special Paper 291, p. 73-81.

Machette, M.N., and Personius, S.F., 1984, Quaternary and Pliocene faults in the eastern part of the Aztec quadrangle and the western part of the Raton quadrangle, Northern New Mexico, U.S. Geological Survey Map MF-1465-B, Scale 1:250,000.

Machette, M.N., Personius, S.F., Kelson, K. I., Dart, R.L., and Haller, K.M., 1998, Map and data for Quaternary faults in New Mexico: U.S. Geological Survey Open-file Report 98-521, 443 pp.

Menges, C.M., 1988, The tectonic geomorphology of mountain front landforms in the northern Rio Grande rift, New Mexico, Albuquerque: [Ph.D. Dissertatin]:, Univ. of New Mexico, Albuquerque, 140 p.

Menges, C.M., 1990, Late Cenozoic rift tectonics and mountain-front landforms of the Sangre de Cristo Mountains near Taos, Northern New Mexico: New Mexico Geological Society, 41st Field Conference, Guidebook, p. 113-122.

Muehlberger, W.R., 1979, The Embudo fault between Pilar and Arroyo Hondo, New Mexico: An active intracontinental transform fault: New Mexico Geological Society, 30th Field Conference, Guidebook, p. 77-82.

Olig, S.S., Kelson, K.I., Gardner, J.N., Reneau, S.L., and Hemphill-Haley, M.A., 1996, The seismic potential of the Pajarito fault system, New Mexico: New Mexico Geological Society, 47th Field Conference, Guidebook, p. 143-151.

Personius, S.F., and Machette, M.N., 1984, Quaternary faulting in the Taos Plateau region, northern New Mexico: New Mexico Geological Society, 35th Field Conference, Guidebook, p. 83-90.

Rosendahl, B.R., 1987, Architecture of continental rifts with special reference to East Africa: Annual Review of Earth and Planetary Sciences, v. 15, p. 445-503.

Russell, L. R. and Snelson, S., 1994, Structure and tectonics of the Albuquerque Basin segment of the Rio Grande rift-- Insights from reflection seismic data: Geological Society of America Special Paper 291, p. 83-112.

Salyards, S.L., Ni, J.F., and Aldrich, M.J., Jr., 1994, Variation in paleomagnetic rotations and kinematics of the north-central Rio Grande rift, New Mexico: Geological Society of America Special Paper 291, p. 59-72.

Steinpress, M.G., 1981, Neogene stratigraphy and structure of the Dixon area, Española basin, north-central New Mexico; Summary: Geological Society of America Bulletin, v. 92, p. 1023-1026.

Wells, D.L., and Coppersmith, K.J., 1994, New empirical relationships among magnitude, rupture length, rupture width, rupture area, and surface displacement: Bulletin of Seismological Society of America, v. 84, no. 4, p. 974-1002.

Wong, I., Kelson, K., Olig, S., Bott, J., Green, R., Kolbe, T., Hemphill-Haley, M., Gardner, J., Reneau, S., and Silva, W., 1996, Earthquake potential and ground shaking hazard at the Los Alamos National Laboratory, New Mexico: New Mexico Geological Society, 47th Field Conference, Guidebook, p 135-142.